#3935

valve/flash tank as a "black box" in which feedwater enters and steam leaves. The feedwater mass flow rate must equal the steam mass flow rate. The feedwater typically enters the tank at a temperature somewhat below the saturation temperature, so that the solar system provides two heating steps. First, the feedwater is heated to saturation, and then the saturated water is vaporized into saturated steam. The solar system energy collection rate is therefore related to the feedwater (or steam) mass flow rate as

$$\dot{Q}_c = \dot{M}_f[c_{pw}(T_s - T_f) + h_{fg}], \tag{12}$$

Equation (12) can be written in terms of the feedwater mass flow rate as

$$\dot{M}_f = \frac{\dot{Q}_c}{c_{pw}(T_s - T_f) + h_{fg}}. \tag{13}$$

The flow stream feeding the collectors is made up of two mixed flow streams. One flow stream is the feedwater and the other is recirculated water from the flash tank:

$$\dot{M}_c = \dot{M}_f + \dot{M}_r, \tag{14}$$

or

$$\dot{M}_r = \dot{M}_c - \dot{M}_f, \tag{15}$$

The temperature of the fluid entering the collectors $T_{c,i}$ is the mixed stream temperature:

$$T_{c,i} = \frac{\dot{M}_f T_f + \dot{M}_r T_r}{\dot{M}_c}. \tag{16}$$

Substituting equation (15) and equation (13) into equation (16), the collector inlet temperature can be written as

$$T_{c,i} = \frac{\dot{Q}_c/\dot{M}_c}{c_{pw}(T_s - T_f) + h_{fg}} T_f + \left[1 - \frac{\dot{Q}_c/\dot{M}_c}{c_{pw}(T_s - T_f) + h_{fg}}\right] T_s. \tag{17}$$

Solving equation (17) for $\dot{Q}_c$, we have

$$\dot{Q}_c = \frac{1}{1 - \dfrac{F_R U_L A_c/\dot{M}_c}{c_{pw}(T_s - T_f) + h_{fg}}(T_s - T_f)} [F_R \eta_o I_a A_c - F_R U_L A_c (T_s - T_a)] \tag{18}$$

The last term in brackets in equation (18) is, as before, the energy collection rate if the fluid that returns to the collector is always at the steam saturation temperature. The first term is the performance enhancement factor of the flash steam system F_F. Note that this term is unity or larger because the mixed stream temperature to the collectors is at or below the steam saturation temperature.

Equation (18) thus be written as

$$Q_c = F_F[F_R \eta_o I_a A_c - F_R U_L (T_s - T_a)]$$

where

$$F_F = \left[1 - \frac{F_R U_L A_c/\dot{M}_c}{c_{pw}(T_s - T_f) + h_{fg}}(T_s - T_f)\right]^{-1} \tag{19}$$

Note that F_F depends only on fixed collector characteristics, industrial process temperatures, water properties, and the collector loop flow rate.

Acknowledgments

This paper presents the derivation of steam system heat exchange factors that were developed during preparation of an IPH design handbook [4] for the U.S. Department of Energy. The support of the D.O.E. as well as the IPH design handbook coauthors is gratefully acknowledged.

References

1 Alvis, R. L., editor, *Proceedings of the Distributed Solar Collector Summary Conference—Technology and Applications*, SAND83-0137C, Sandia National Laboratories, Albuquerque, N.Mex., Mar. 1983.

2 deWinter, F., "Heat Exchanger Penalties in Double-Loop Solar Water Heating Systems," *Solar Energy*, Vol. 17, 1975, p. 335.

3 May, E. K., and Murphy, L. M., "Performance Benefits of the Direct Generation of Steam in Line-Focus Solar Collectors," ASME JOURNAL OF SOLAR ENERGY ENGINEERING, Vol. 105, May 1983, p. 126.

4 Kutscher, C. F., Davenport, R. L., Dougherty, D. A., Gee, R. C., Masterson, P. M., and May, E. K., "Design Approaches for Solar Industrial Process Heat Systems." *SERI/TR-253-1356*, Aug. 1982, Solar Energy Research Institute, Golden, CO.

Verification of a Numerical Simulation Technique for Natural Convection[1]

A. Gadgil,[2] F. Bauman,[2] E. Altmayer,[2] and R. C. Kammerud[2]

Nomenclature

A = aspect ratio, H/L
Gr = Grashof number, $g\beta\Delta TH^3/\nu^2$
g = acceleration of gravity
H = enclosure height
$\hat{j}$ = unit vector in direction of gravity
k = thermal conductivity
L = enclosure length
Nu = Nusselt number $q_{avg}H/(\Delta T\, k)$
p = dimensionless pressure, $p^*H^2/\rho\nu^2$
Pr = Prandtl number, ν/α
q_{avg} = average heat flux at the hot wall
q_{loc} = local heat flux along the hot wall
Ra = Rayleigh number, $g\beta\Delta TH^3 Pr/\nu^2$
T = temperature
T_c = cold wall temperature
T_h = hot wall temperature
T_m = mean fluid temperature, $(T_h + T_c)/2$
V = dimensionless velocity, v^*H/ν
X = dimensionless horizontal distance, x^*/H
Y = dimensionless vertical distance y^*/H
α = thermal diffusivity
β = coefficient of thermal expansion
ΔT = $(T_h - T_c)$
θ = dimensionless temperature, $(T - T_m)/\Delta T$
ν = kinematic viscosity
ρ = fluid density

Superscripts

$*$ = dimensional quantities

[1] This work was supported by the Assistant Secretary for Conservation and Renewable Energy, Office of Solar Heat Technologies, Passive and Hybrid Solar Energy Division, of the U.S. Department of Energy under Contract No. DE-AC03-76SF00098.

[2] Passive Research and Development Group, Lawrence Berkeley Laboratory, University of California, Berkeley, Calif. 94720

Contributed by the Solar Energy Division for publication in the JOURNAL OF SOLAR ENERGY ENGINEERING. Manuscript received by the Solar Energy Division, May 14, 1983.

Introduction

Among the fundamental heat transfer processes in buildings, convection is the least understood. In contrast to conduction and radiation, the equations governing convective heat and mass transfer in fluids, that is, the continuity, momentum, and energy equations, do not have closed solutions even under steady-state conditions. During recent years, considerable attention has been given to both experimental and numerical investigations of natural convection in enclosures. A number of review papers [1, 2] have been published, although a majority of the reported studies cover a range of Rayleigh numbers ($Ra < 10^8$) and aspect ratios ($H/L > 1$), which are not typical of buildings. Most recently, de Vahl Davis [3, 4] has performed a comparison study between a large number of numerical methods for laminar natural convection in a square cavity.

To develop an improved understanding of convection in buildings, a coordinated analytic and experimental effort has been undertaken at Lawrence Berkeley Laboratory. A computer program (CONVEC2) has been developed that numerically simulates two-dimensional natural convection in rectangular enclosures at Rayleigh numbers on the order of 10^{10}. Small-scale experiments have been carried out [5, 6] to provide for (*a*) verification of the numerical analysis, and (*b*) development of empirical heat transfer correlations for a few enclosure configurations. Once it has been carefully verified against experiments, CONVEC2 can be used to simulate convection processes occurring in a broad range of enclosures for a variety of boundary conditions. From this numerically generated heat transfer "data base," engineering correlations can be developed [7].

The present paper describes a verification of CONVEC2 for single-zone geometries by comparison with the results of two natural convection experiments [6, 8] performed in small-scale rectangular enclosures. These experiments were selected because of the high Rayleigh numbers obtained ($2.6 \times 10^8 \leq Ra \leq 1.3 \times 10^{10}$) and the small heat loss (<5 percent) through the insulated surfaces. Comparisons are presented for (*i*) heat transfer rates, (*ii*) fluid temperature profiles, and (*iii*) surface heat flux distributions.

Computer Code Description

A computer program, CONVEC2, which solves the governing equations for fluid motion in two-dimensional enclosures, has been developed. This program is based on the finite-difference method, which divides the volume of interest into a set of subvolumes; the time is also divided into discrete time-steps. The computations employ the Patankar-Spalding hybrid-differencing scheme [9]. The time-dependent differential equations are integrated over the finite number of subvolumes and over each time-step to obtain a large number of simultaneous algebraic equations, which are solved by matrix inversion. This procedure is repeated for successive time-steps until the fractional residues of the velocity and temperature fields are less than 10^{-4}. The solutions yield the fluid temperatures and velocities at the grid-nodes, each of which is centered within one subvolume. The computer program uses variable grid spacing to achieve high resolution in regions of rapidly changing flow. The program methodology is described in detail in [10].

The governing equations for steady-state laminar flow of a fluid with Boussinesq[3] approximation are:

$$\text{Continuity:} \quad \nabla \cdot \mathrm{V} = 0 \tag{1a}$$

$$\text{Momentum:} \quad (\mathrm{V} \cdot \nabla)\mathrm{V} = \nabla^2 \mathrm{V} - \nabla P + Gr\hat{j}\theta \tag{1b}$$

$$\text{Energy:} \quad (\mathrm{V} \cdot \nabla)\theta = (1/Pr)\nabla^2\theta \tag{1c}$$

[3] Under the Boussinesq approximation, the effect of variable fluid density is incorporated into the buoyancy producing term of the momentum equation.

The temperature or heat-flux profiles are specified for vertical and horizontal walls along with no-slip velocity boundary conditions on all enclosure surfaces.

CONVEC2 is suitable for modeling both natural and forced convection in two dimensions, for internal and external flows. In addition, the program can model any combination of obstacles (internal partitions, furniture, building exteriors), heat sources and sinks (space heating and cooling), and velocity sources and sinks (fans, windows). In addition to the results presented herein, comparisons of CONVEC2 with other experimental and analytical work on high Ra enclosure convection have previously been reported [5, 11, 12].

Experimental Overview

Figure 1 shows a cross-sectional schematic diagram of the configuration used in the two small-scale experiments [6, 8]. One vertical wall is heated to a constant temperature, T_h, and the opposite vertical wall is cooled to a constant temperature, T_c. The horizontal surfaces (floor and ceiling) are adiabatic. The apparatus used by Nansteel and Greif [6] had an aspect ratio, $A = H/L = 0.5$, while Righi [8] used $A = 0.2$. Both of the experiments used water as the working fluid and both investigated heat transfer at relatively large values of Rayleigh number $2.9 \times 10^9 \leq Ra \leq 1.3 \times 10^{10}$ [6] and $2.6 \times 10^8 \leq Ra \leq 4.7 \times 10^9$ [8]).

The experimental configuration and conditions described in the foregoing are particularly well suited for the investigation of convective heat transfer in passive solar buildings as well as for verification of CONVEC2 for the following reasons.

(1) Aspect ratios in the range of 0.2 to 0.5 are representative of room geometries.

(2) The thermal boundary conditions are representative of typical passive solar configurations; for example, they are analogous to heat input from a warm interior thermal storage wall and heat loss through a cold exterior window in an otherwise well-insulated room.

(3) The high values of Rayleigh number are representative of those values encountered in full-scale buildings; the Rayleigh numbers will always be greater than 10^9.

(4) The opacity of water to thermal radiation allows for the measurement of the purely convective component of heat transfer across the enclosure; the resulting data were therefore ideally suited for comparison with the predictions of CONVEC2.

Due to Prandtl number differences, the results of experiments using water as the working fluid are not directly applicable to the problem of convection of air in full-scale buildings. For this application, the predictions of CONVEC2 are needed.

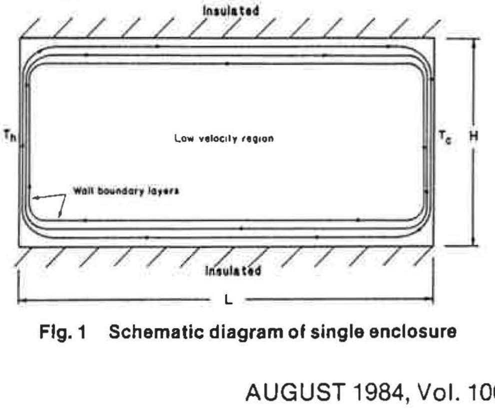

Fig. 1 Schematic diagram of single enclosure

range of temperatures encountered in the experiments (2.57×10^{-4} °C^{-1} $\leq \beta \leq 4.91 \times 10^{-4}$°C^{-1} and 5.2×10^{-7} m^2/sec $\leq \nu \leq 9.1 \times 10^{-7}$ m^2/sec).

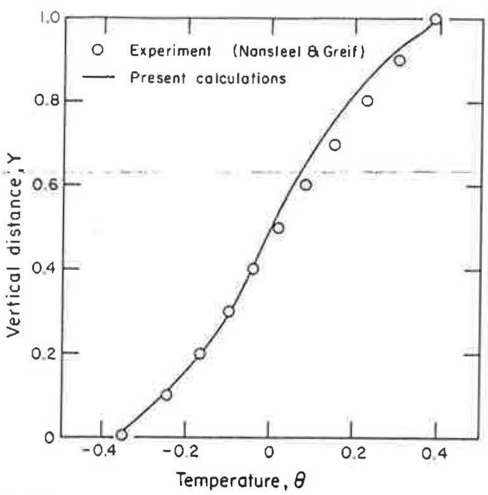

Fig. 2(a) Vertical centerline ($x/L = 0.5$) temperature profile, $Ra = 1.3 \times 10^{10}$, $Pr = 3.1$, $A = H/L = 0.5$

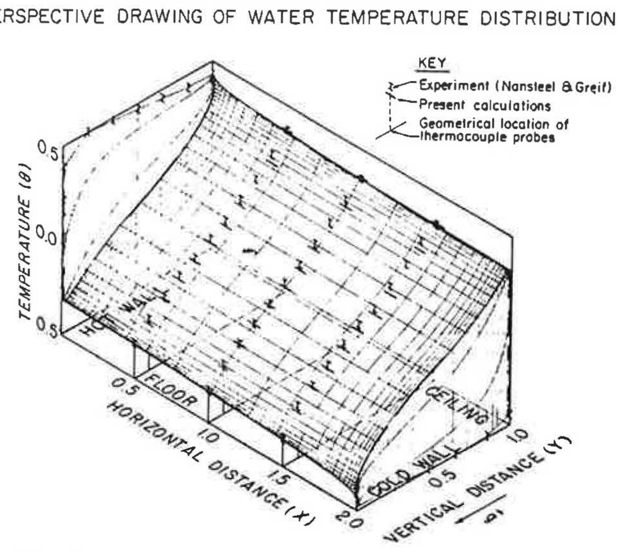

Fig. 2(b) Comparison of experimental data and numerical predictions of water temperature distribution, $Ra = 1.3 \times 10^{10}$, $Pr = 3.1$, $A = H/L = 0.5$

Fig. 2

Although indications of the onset of transitional flow have been observed at the highest Rayleigh number (1.3×10^{10}) of the present study, three separate experimental studies [6, 13, 14] of high Ra convection in enclosures report no evidence of full turbulence at this Ra value. Thus the laminar flow equations, equations (1a-c), are assumed to be applicable for the comparisons presented in the following.

Results and Discussion

To carry out the validation, the laminar flow equations, (1$a-c$), were solved numerically for ($2.6 \times 10^8 \leq Ra \leq 1.3 \times 10^{10}$) using CONVEC2. A study of the sensitivity of boundary layer profiles to grid size led to the choice of a variable-spaced grid of 31×35 nodes in x and y directions, respectively. Typically, each simulation required 700 sec of execution time on a CDC 7600 computer.

The numerical heat transfer results for both experiments were generated under the assumption of adiabatic horizontal surfaces. All numerical simulations assumed constant properties of water, evaluated at the mean fluid temperature, $(T_h + T_c)/2$. The comparisons indicate good agreement despite the fact that water fluid properties will vary over the range of temperatures encountered in the experiments (2.57×10^{-4} °C^{-1} $\leq \beta \leq 4.91 \times 10^{-4}$°C^{-1} and 5.2×10^{-7} m^2/sec $\leq \nu \leq 9.1 \times 10^{-7}$ m^2/sec).

Fluid Temperature Distribution. In Fig. 2(a) the numerically predicted and experimentally measured vertical centerline temperature profiles (at $X = 1.0$) are compared for the highest value of Rayleigh number ($Ra = 1.3 \times 10^{10}$) obtained in [6]. For this simulation the measured horizontal surface temperature boundary conditions were input to CONVEC2. The agreement is seen to be quite good, particularly in the lower half of the enclosure. In the upper portion of the enclosure, where the largest differences are observed (2°C = 3.5 percent error, relative to ΔT = 56.7°C for this simulation), the influence of variable fluid (water) properties (requiring the Boussinesq approximation to be dropped), when included in future numerical calculations, may improve the agreement.

To more clearly visualize the characteristics of the water temperature distribution throughout the enclosure, a three-dimensional perspective drawing (with temperature as the third dimension) is shown in Fig. 2(b). This computer-generated drawing is based on the results of the highest Rayleigh number simulation described in the foregoing. The experimentally measured [6] vertical temperature profiles at three different horizontal locations (X = 0.5, 1.0, 1.5) are also indicated in the drawing by error bars (±1°C). The horizontal slash near each experimental bar depicts the point at which the numerically predicted temperature "surface" is penetrated by the projection line of the corresponding thermocouple probe location. Again, the numerical and experimental results agree at all points to within 3.5 percent of ΔT for this simulation. The grid lines shown in Fig. 2(b) represent the actual variable-spaced grid of 31×35 nodes used by CONVEC2 during the simulations.

Several observations can be made regarding the water temperature distribution shown in Fig. 2(b). Near the two vertical walls, where strong natural convection boundary layers[4] have developed along the heat transfer surfaces, extremely large horizontal temperature gradients are evident. On the other hand, in the central core region where very low fluid velocities exist, the fluid temperature exhibits virtually no variation across the entire horizontal distance between the two vertical boundary layers. The nearly linear slope of the temperature "surface" in the vertical direction displays the stable stratification of the water in this core region. The fact that the central core region extends to within a distance of X=0.024 from the vertical walls demonstrates the extremely thin vertical boundary layers along these surfaces. The small temperature inversion immediately outside of the vertical boundary layers, as analytically predicted in [11], is noticeable in the figure as the apparent discontinuities in the horizontal grid lines. Figure 2(b) also shows the temperature variation along all four enclosure surfaces, which matches the experimentally measured temperature distribution.

Heat Transfer Results. Numerical results for the Nusselt number are compared with the experimentally obtained values of reference [6] in Fig. 3(a) for an enclosure with aspect ratio, A = 0.5. The agreement is seen to be very good even at the highest value of the Rayleigh number of 1.3×10^{10}. The largest observed difference between numerical and experimental data points is only 5 percent.

In Fig. 3(b) the Nusselt numbers predicted by CONVEC2 are compared with the experimental values of reference [8] for an enclosure with aspect ratio, A = 0.2. The agreement is excellent for Rayleigh numbers below 2×10^9. The largest

[4] At the mid-height along the hot wall, the numerically predicted maximum vertical component of the water velocity was 2.6 m/sec, with a boundary layer thickness of 2.3 mm.

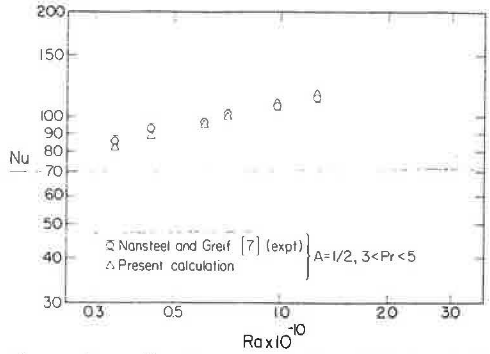

Fig. 3(*a*) Comparison of heat transfer results at high *Ra*, $A = H/L = 0.5$, water

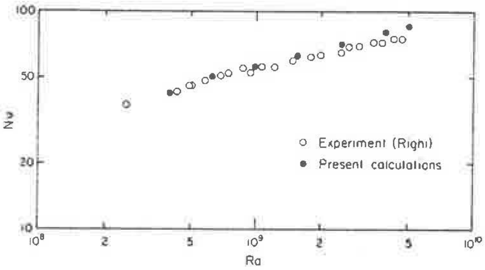

Fig. 3(*b*) Comparison of heat transfer results at high *Ra*, $A = H/L = 0.2$, water

Fig. 3

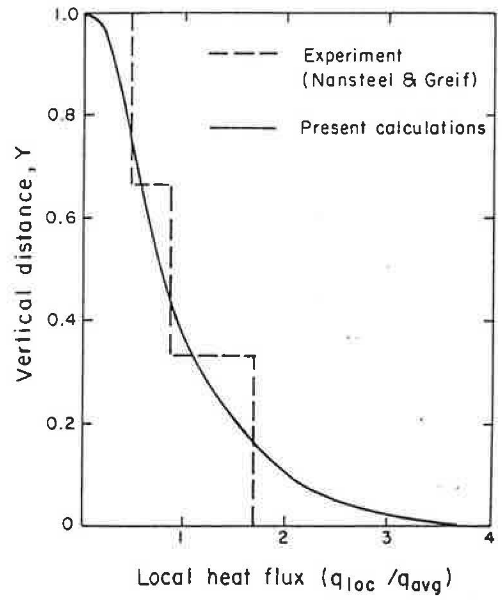

Fig. 4 Hot wall heat flux distribution, $Ra = 1.3 \times 10^{10}$, $Pr = 3.1$, $A = H/L = 0.5$

observed difference is 10 percent near a Rayleigh number of 5 $\times 10^9$.

Hot Wall Heat Flux Distribution. The numerically predicted heat flux distribution along the fluid side of the hot wall is compared in Fig. 4 with the experimentally measured heat flux [6] supplied by the heaters to the outer surface of the hot wall. In the experiment there were three independently controlled and monitored horizontal strips of thermofoil heaters, each having a height of $Y = 0.33$. The discontinuities in the experimental heat flux profile shown in Fig. 4 are therefore an artifact of limitations in the measurement technique. In reality, vertical conduction through the copper hot wall (4.8 mm thick) would tend to smooth out the heat flux profile. Although no quantitative comparison can be made between the two profiles, the numerically obtained heat flux profile approximates a smoothed-out heat flux profile quite well.

Conclusions

The numerical predictions of a computer program (CONVEC2) have been compared with results from two experimental investigations of laminar natural convection in enclosures at high Rayleigh numbers. The agreement for both heat transfer and fluid temperature data is excellent even at the highest Rayleigh number studied ($Ra = 1.3 \times 10^{10}$). Qualitative agreement is also seen to be good for the hot wall heat flux distribution. The results indicate that CONVEC2 is capable of accurately simulating high Rayleigh-number, laminar natural convection in enclosures of aspect ratio slightly less than one, having warm and cold surfaces on opposite vertical walls.

The results of experiments using water-filled enclosures such as those previously described are not directly applicable (due to Prandtl number differences) to the problem of air convection in full-scale buildings. However, they can effectively be used for verification of the computer program CONVEC2. The verified program can in turn be used to examine convective heat transfer in air-filled enclosures. As long as the appropriate values of room aspect ratios, surface temperature boundary conditions, and Rayleigh and Prandtl numbers are employed during the simulations, heat transfer and temperature predictions for air in full-scale buildings can be obtained with the same accuracy as has been demonstrated in the comparisons presented in this paper.

References

1 Ostrach, S., "Natural Convection in Enclosures," in *Advances in Heat Transfer*, Irvine, T. F., Jr., and Hartnett, J. P., eds., Vol. 8, 1972, Academic Press, New York, pp. 161-227.

2 Catton, I., "Natural Convection in Enclosures," *Proceedings, 6th International Heat Transfer Conference*, Toronto, Canada, Vol. 6, 1978, pp. 13-31.

3 de Vahl Davis, G., "Natural Convection in a Square Cavity: A Comparison Exercise," in *Proceedings of the 2nd International Conference on Numerical Methods*, Venice, Italy, 1981. (Also Report No. 1982/FMT/3, School of Mechanical and Industrial Engineering, University of New South Wales.)

4 de Vahl Davis, G., "Natural Convection in a Square Cavity: A Bench Mark Numerical Solution," in *Proceedings of the 2nd International Conference on Numerical Methods*, Venice, Italy, 1981; (also available as Report No. 1982/FMT/2, School of Mechanical and Industrial Engineering, University of New South Wales).

5 Bauman, F., Gadgil, A., Kammerud, R., and Greif, R., "Buoyancy Driven Convection in Rectangular Enclosures: Experimental Results and Numerical Calculations," ASME paper No. 80-HT-66. (Also Lawrence Berkeley Laboratory Report LBL-10257, 1980.)

6 Nansteel, M., and Greif, R., "Natural Convection in Unidivided and Partially Divided Rectangular Enclosures," ASME *Journal of Heat Transfer*, Vol. 103, 1981, pp. 623-629.

7 Altmayer, E., Gadgil, A., Bauman, F., and Kammerud, R., "Correlations for Convective Heat Transfer From Room Surfaces," *ASHRAE Transactions*, Vol. 89:2A, 1983, pp. 61-77. (Also Lawrence Berkeley Laboratory Report, LBL-14893, 1983.)

8 Righi, J., "Physical Experiments on Free Convection in a Tilted Rectangular Enclosure of Aspect Ratio 0.2," Report No. MIE-062 NSF-ENG77-08441), Clarkson College, Potsdam, N.Y.

9 Patankar, S. V., and Spalding, D. B., *Heat and Mass Transfer in Boundary Layers*, Morgan-Grampion Books, Ltd., London, 1967.

10 Gadgil, A., "On Convective Heat Transfer in Building Energy Analysis," Ph.D. Dissertation, Department of Physics, University of California, Berkeley, 1979. (Also Lawrence Berkeley Laboratory Report, LBL-10900, 1980.)

11 Tichy, J., and Gadgil, A., "High Rayleigh Number Laminar Convection in Low Aspect Ratio Enclosures With Adiabatic Horizontal Walls and Differentially Heated Vertical Walls," ASME *Journal of Heat Transfer*, Vol. 104, 1982, pp. 103-110.

12 Shiralkar, G., Gadgil, A., and Tien, C. L., "High Rayleigh Number Convection in Shallow Enclosures With Different End Temperatures," *Int. J. of Heat and Mass Transfer*, Vol. 24, 1981, pp. 1621-1629.

13 Hess, C., and Henze, R., "Experimental Investigation of Natural Convection Losses from Open Cavities," *J. of Heat Transfer*, in press. (Also Sandia Laboratory Report No. SAND 81-8014.)

14 Bohn, M., Olson, D., and Kirkpatrick, A., "Experimental Study of Three-Dimensional Natural Convection at High Rayleigh Numbers," ASME Paper No. 83-HT-12.